Published in final edited form as:
Cancer J. 2015 ; 21(2): 129–136. doi:10.1097/PPO.0000000000000105.

Imaging Tumor Metabolism Using Positron Emission Tomography

David Y. Lewis[1], **Dmitry Soloviev**[1], and **Kevin M. Brindle**[1]

[1]Cancer Research UK - Cambridge Institute, University of Cambridge, Li Ka Shing Centre, Cambridge, UK

Abstract

Positron emission tomography (PET) is an extraordinarily sensitive clinical imaging modality for interrogating tumor metabolism. Radiolabelled PET substrates can be traced at sub-physiological concentrations, allowing non-invasive imaging of metabolism and intra-tumoral heterogeneity in systems ranging from advanced cancer models to cancer patients in the clinic. There are a wide range of novel and more established PET radiotracers, which can be used to investigate various aspects of tumor metabolism, including carbohydrate, amino acid and fatty acid metabolism. In this review we will briefly discuss the more established metabolic tracers and describe recent work on the development of new tracers. Some of the unanswered questions in tumor metabolism will be considered alongside new technical developments, such as combined PET/MRI machines, that could provide new imaging solutions to some of the outstanding diagnostic challenges facing modern cancer medicine.

Introduction

Positron emission tomography (PET) is an extraordinarily sensitive clinical imaging modality for interrogating tumor metabolism [1]. The main strength of PET is that radiolabelled substrates can be traced at sub-physiological concentrations and can, therefore, be used to measure metabolic fluxes without the perturbation resulting from injection of a large chemical load [2]. High sensitivity also permits rapid imaging for dynamic assessment of tumor uptake and washout of the labeled metabolite(s). Since only the radiolabel is detected, and there is no information about the chemical species in which the label is incorporated, PET imaging often needs to be accompanied by careful investigation of the circulating radiolabelled metabolites. The ideal PET tracer would be irreversibly incorporated into a single cell metabolite or compartment that detects some specific feature of cancer cell metabolism and which can be separated, either spatially or temporally in the resulting images, from non-cancer specific processes. The metabolic processes that are aberrant in cancer and which can be exploited for PET imaging include elevated glycolysis [1], amino acid uptake [3], protein synthesis [4], fatty acid synthesis [5, 6] and nucleotide synthesis associated with increased cell proliferation [7] (see Figure 1). Metabolite pools

Corresponding Author: Prof. Kevin M. Brindle FMedSci, Department of Biochemistry, University of Cambridge, Tennis Court Road, Cambridge CB2 1GA and Cancer Research UK Cambridge Institute, Li Ka Shing Centre, Robinson Way, Cambridge, CB2 0RE, Phone +44 (0)1223 333674 or 769647, Fax +44 (0)1223 766002 or 769510, kmb1001@cam.ac.uk.

Europe PMC Funders Author Manuscripts

that show transient labeling can be interrogated, and metabolic fluxes can be derived from PET images by using dynamic imaging, with rapid blood sampling and pharmacokinetic modeling; something which is arguably still lacking in maturity for oncological applications of PET [8, 9].

A wide range of new and classical PET radiotracers have been used in preclinical and clinical investigations and while it is unlikely that many of the new agents will transfer into routine clinical practice it is nevertheless plausible some of them will be useful for clinical decision making in the future [10]. The majority will most likely be used in a research setting, ideally in combination with other imaging modalities such as MRI, to better understand cancer metabolism [11] and to facilitate the drug development process by giving an early indication of drug efficacy in early stage clinical trials [2, 7, 12]. A list of some metabolic PET tracers, classed by the metabolic pathway that they interrogate, is shown in Table 1. A comprehensive molecular imaging tracer database is available online from the NCBI [13]. In this review we will briefly present the classical metabolic PET tracers and describe recent work on the development of new tracers.

Carbohydrate utilization and storage

Indisputably the most important PET tracer for imaging tumor metabolism is 2-[^{18}F]fluoro-2-deoxy-D-glucose (FDG). It is over three decades since the first images of a tumor accumulating FDG were published [14] and FDG remains the archetypal PET tracer for tumor characterization, staging and response evaluation. Tumors, unlike normal tissues, show high rates of aerobic glycolysis, which as well as providing ATP, also provides glycolytic intermediates that are used in anabolic pathways for the synthesis of amino acids, lipids, nucleotides and NADPH [15]. FDG is widely recognized as a tracer for imaging the Warburg effect in cancer [16], that is up regulated glucose utilization in the presence of oxygen, where the pyruvate generated by the glycolytic pathway is not oxidized in the mitochondria but rather reduced to lactate [17, 18].

While it seems inconceivable that the dominance of FDG as the PET agent for tracing cancer carbohydrate metabolism will be surpassed, not all tumors are FDG avid and FDG is not always cancer specific, for example there can be increased FDG uptake in inflammation [19].

A number of attempts have been made to develop ^{18}F-labelled PET analogues from other sugars, including D-mannose [20], D-lactose [21], D-fructose [22] and D-galactose [23]. Of these 1-[^{18}F]fluoroethyl-β-D-lactose (FEL) has shown promise in delineating peritumoural regions of pancreatic cancer that overexpress hepatocarcinoma-intestine-pancreas/pancreatitis-associated protein (HIP/PAP) [21]. [^{18}F]FEL binds to the carbohydrate-binding domain of HIP/PAP with higher affinity than other sugars and HIP/PAP is highly overexpressed in the peritumoural region compared to normal pancreas and chronic pancreatitis [24, 25]. 6-deoxy-6-[^{18}F]fluoro-D-fructose ([^{18}F]FDF) is transported into the cell by the glucose transporter, GLUT-5, and subsequently phosphorylated by a ketohexokinase, unlike FDG which is transported predominantly by GLUT-1 and GLUT-3 in tumors and phosphorylated by hexokinase [22, 26]. [^{18}F]FDF therefore detects a pathway

that is distinct from that used by glucose and which may predominate in some forms of breast cancer [22], although the role of GLUT-5 in cancer is not yet established [27].

FDG reports on the first two steps in the glycolytic pathway – plasma membrane transport and subsequent phosphorylation by hexokinase [28]. A novel probe for imaging glycogen metabolism (glycogenesis) has been described recently that reports on several steps in the glycogen synthesis pathway [29]. Uptake of [^{18}F]-N-(methyl-(2-fluoroethyl)-1H-[1,2,3]triazole-4-yl)glucosamine ([^{18}F]NFTG) was determined principally by glycogen synthase 1 levels, which were shown to be high during cellular quiescence [30]. The mechanism responsible for tracer accumulation remains to be elucidated, however a possible route is via galactokinase 1 (GALK1), galactose 1-phosphate uridylyltransferase (GALT), UDP-galactose epimerase (GALE) and glycogen synthase 1 (GYS1) [31].

The pentose phosphate pathway (PPP) is an important component of cellular carbohydrate metabolism, responsible for the synthesis of nucleotides and the generation of biosynthetic reducing power in the form of NADPH. However, the complex regulation of the PPP in cancer is still not fully understood [32]. The recent development of [^{18}F]-2-deoxy-2-fluoroarabinose has shown that this modified ribose is transported by GLUT-2, phosphorylated by ribokinase and further metabolized by transketolase, the latter being a key enzyme in the PPP. Although developed as a probe of the ribose salvage pathway this radiotracer may also prove useful for studying aspects of PPP activity in vivo [33].

Amino Acids

Numerous amino acids have been radiolabelled for imaging flux through various amino acid transporters and in some cases for measuring protein synthesis [3]. Protein synthesis rates have been measured in muscle using [^{11}C]methionine [34], in normal brain using [^{11}C]leucine [35], in soft tissue sarcoma [36] and pituitary adenoma [37] using [^{11}C]tyrosine, and in glioma using [^{11}C]tyrosine and [^{11}C]methionine [4, 38]. Radiolabeled unnatural amino acids can be used to visualize amino-acid transporter activity specifically as they are not recognized by aminoacyltRNA synthetases and therefore not incorporated into proteins [3]. Numerous amino acid transporter subtypes have been described with varying substrate specificities (denoted as type A, B^0, N, ASC, X-AG, L, y^+, y^+L, x_c^-). Typical tracers include L-type amino acid transporter substrates such as [^{18}F]fluoroethyltyrosine ([^{18}F]FET) and [^{18}F]-dihydroxy-phenyl-alanine ([^{18}F]FDOPA) [39, 40], which have been used for cancer diagnosis and for monitoring treatment response in tumors that are difficult to image with FDG, especially brain tumors. L-type amino acid transporter 1 (LAT1) expression is increased in glioma and many other cancers and is associated with high grade and poor prognosis [41-44]. [^{18}F]FET has been reported to be useful not only for visualizing tumors, but also for grading, monitoring treatment response and differentiating pseudoprogression from early treatment failure in glioblastoma [45-47].

Recently efforts have been made to radiolabel substrates of other amino acid transporters, in addition to LAT1. ASCT2, like LAT1, is an obligatory amino acid exchanger whose expression is prognostic in pancreatic and non small cell lung cancer (NSCLC) [48, 49]. ASCT2 and LAT1 may co-operate during malignant transformation to generate an influx of

glutamine, and other amino acids, for the biosynthetic processes that support tumor growth and cancer cell survival [50]. The leucine analogue trans-1-amino-3-[^{18}F]fluorocyclobutanecarboxylic acid (FACBC) is transported by ASCT2 and LAT1 and has shown high tumor uptake and low bladder excretion in a number of clinical studies of prostate cancer [51, 52].

System A amino acid transporters (SNAT 1, 2 and 4) are electrogenic and concentrative and therefore potentially attractive targets for PET. The recently described agents (R)- and (S)-3-[^{18}F]Fluoro-2-Methyl-2-N-(Methylamino)propanoic Acid ([^{18}F]FMeAMP) are transported predominantly by A type amino acid transporters and showed up to 115 times more uptake in 9L rat glioma cells compared to normal brain. However this ratio was enhanced by a lack of type A transporters on the luminal membranes of blood vessels in normal brain (in the tumor there is breakdown of the blood brain barrier (BBB) [53]) and therefore [^{18}F]FMeAMP uptake in the glioma measures predominantly BBB breakdown rather than cerebral amino acid uptake *per se*. The tracer may be more suitable, therefore, for tumors originating at other sites. Uptake of [^{18}F]FMeAMP was recently observed in breast, NSCLC, prostate and ovarian cancer xenografts [54].

Three new tracers that are specific for system x_c^- transporters have been described; ^{18}F-5-fluoro-L-aminosuberic acid ([^{18}F]FASu) [55], [^{18}F]-(2S,4S)-4-Fluoroglutamate [56, 57] and [^{18}F](2S,4S)-4-(3-Fluoropropyl)glutamate ([^{18}F]FSPG) [58], with uptake of the latter demonstrated in hepatocellular carcinoma [59], and in NSCLC and breast cancer patients [60]. System $x_c^-$is an electroneutral cystine/glutamate antiporter. System x_c^- activity directly regulates the concentration of glutathione, an intracellular antioxidant peptide, as uptake of cystine and its subsequent reduction to cysteine are rate-limiting steps for glutathione synthesis [61]. System xc^- is up regulated under conditions of oxidative stress, which increases glutathione production and protects the cell from oxidative damage [62]. Since chemoresistant cancer stem cells stabilize system x_c^- activity, increasing their capacity to withstand oxidative stress [63], imaging system x_c^- activity may be predictive of resistance to treatment [62].

Some tumors use glutamine preferentially for anaplerosis and energy production (glutaminolysis), which can be activated by oncogenic *myc* signaling [17, 64]. A series of PET tracers have been designed to image glutaminolysis including L-[5-^{11}C]-glutamine [65, 66], [^{18}F]-(2S,4R)-4-Fluoroglutamine ([^{18}F]FGln) [57, 67, 68] and [^{18}F](2S,4S)-4-(3-Fluoropropyl)glutamine ([^{18}F]FPGln) [69]. Initial evaluation of these tracers showed high uptake in rat gliosarcoma 9L xenografts and retention in pancreas, liver and muscle. [^{18}F]FGln and L-[5-^{11}C]-glutamine, but not [^{18}F]FPGln, were incorporated into the protein fraction of 9L and SF188 (pediatric glioblastoma) cell lines. Different patterns of uptake were noted between L-[^{3}H]glutamine and the fluorinated analogues [67, 69]. Uptake of [^{18}F]FGln was recently shown in glioma patients with tumor-to-normal brain ratios greater than 4, although [^{18}F]FGln was defluorinated *in vivo* with subsequent skeletal uptake [68]. L-[5-^{11}C]-glutamine and [^{18}F]FGln have some specificity for ASCT2 while [^{18}F]FPGln appears to be transported by LAT1.

Fatty Acids

Fatty acids (FA) are major substrates for catabolic and anabolic processes; cancer cells often showing high levels of lipid droplet formation [70], fatty acid oxidation [71] and *de novo* fatty acid synthesis [72]. FA, labeled with both ^{11}C and ^{18}F, have been developed as PET tracers, mostly for studying β-oxidation [73]. The most promising of these are the thia-substituted fatty acids, which incorporate sulphur in position 4 of the FA carbon chain [74]. These exhibit metabolic stability and trapping subsequent to their commitment to mitochondrial fatty acid oxidation. Of these 18-[^{18}F] fluoro-4-thia-oleate (FTO) showed the highest uptake in the protein-bound fraction in heart, liver and muscle mitochondria [75]. The proposed mechanism for cell accumulation is via entry on the fatty acid transport protein, esterification to produce FTO-CoA and trans-esterification to FTO-carnitine (catalyzed by CPT-1). Subsequent trapping inside the mitochondria occurs after two steps of β-oxidation and spontaneous decomposition to 14-[^{18}F]fluoro-tetradecane-1-thiol, which binds covalently or non-covalently to various mitochondrial proteins. In obese individuals increased FA flux from visceral fat to hepatic oxidation was demonstrated using dynamic PET measurements with [^{11}C]palmitic acid [73].

Tumor cells show increased *de novo* fatty acid synthesis, which is required for rapid proliferation and cell survival [76]. Fatty acid synthase (FASN), a key enzyme in this pathway, has recently come into focus as a potential therapeutic target in cancer [77, 78]. [^{11}C]Acetate can be used to monitor *de novo* fatty acid synthesis in mice [5, 6, 79] and translational studies are ongoing to assess its utility in humans. The major drawback of [^{11}C]acetate as a tracer for monitoring FASN activity is that it is used in both the oxidative and fatty acid synthesis pathways [77, 78] and the half-life of carbon-11 (t½ 20.4 min) may be too short to detect the synthesis component. Attempts have been made to develop a radiotracer labeled with the longer-lived radionuclide fluorine-18 (t½ 109.8 min). The closest analogue [^{18}F]fluoroacetate has been studied *in vivo* [80], however it did not trace the fatty acid synthesis pathway and therefore cannot be used for FASN activity monitoring [81]. Whether another short-chain fatty acid 2-[^{18}F]fluoropropionate is a tracer of *de novo* fatty acid synthesis remains to be determined, but initial studies in prostate tumor xenografts demonstrated high tumor retention [82]. [^{18}F]Fluoropivalic acid was initially developed as a tracer for fatty acid synthesis [83], however its accumulation in murine breast adenocarcinoma cells as the carnitine ester ruled it out as a fatty acid synthesis tracer and instead suggested a potential role as a probe of fatty acid β-oxidation [84].

[^{11}C]Choline, and the fluorinated analogues [^{18}F]fluoromethylcholine and [^{18}F]fluoroethylcholine, have been used extensively for imaging several malignancies but primarily for detection of prostate cancer [85, 86]. The mechanism of choline accumulation in tumors is not fully understood and might reflect either the activity of the *de novo* phosphatidylcholine synthesis (Kennedy) pathway or oxidative metabolism via the betaine-sarcosine-glycine pathway, which was shown recently to be highly active in prostate cancer [87, 88]. To simplify its metabolic profile deuterated versions of radiolabelled choline were developed in order to reduce betaine oxidation whilst preserving phosphorylation and entry into the Kennedy pathway [89, 90]. Clinical translation may provide additional insight into

Europe PMC Funders Author Manuscripts

the nature of malignant transformation in prostate cancer, with first-in-man studies reported recently [91].

Unanswered questions in tumor metabolism

Metabolic reprogramming is one of the hallmarks of cancer and yet the metabolic niches within the tumor microenvironment are still not well understood [92]. There are a number of unanswered questions in cancer metabolism such as the extent of glutaminolysis [17], glycine dependence [93], metabolic symbiosis [94] and de-novo purine synthesis [95]. Tumors can utilize various substrates [96], including acetate [78], lactate [97], glycine [93], glutamine [98] and proline [99]. How does the utilization of these substrates vary between different tumor types and does this confer susceptibility or resistance to certain kinds of therapy?

Some insight into these questions could be gained by quantitative PET imaging, which requires dynamic imaging with arterial metabolite-corrected plasma concentrations as an input function for a well-designed compartmental model [100]. Many of these mathematical models were designed for neuroscience applications, where the BBB tends to exclude circulating radiometabolites. Their use in cancer may require double input functions to control for radiometabolites that re-enter the tumor [8, 101].

Although the energy of the emitted positrons may vary been different radionuclides, two PET tracers injected simultaneously cannot be distinguished in the same scan as the energy of the two γ-rays resulting from positron annihilation, which are what is detected in the PET scanner, is a constant at 511 keV. Therefore measurements with dual radiotracers need to be performed sequentially. One possibility would be to use a single PET tracer for measuring several distinct processes. For example in separate studies [^{11}C]acetate has been used with modeling approaches to measure blood flow [102], oxidation [103] and fatty acid synthesis [5, 104], all of which are altered within a tumor and potentially provide prognostic information.

One of the challenges will be in validating new tracers as few complementary techniques are available. One possibility would be to measure uptake and flux through a particular pathway with the same substrate labeled in different preparations with ^{11}C and hyperpolarized ^{13}C [105-107]. These could be imaged simultaneously with magnetic resonance spectroscopic imaging (MRSI) and PET in a combined PET/MRI scanner [108]. In addition to the logistical challenges of such an experiment, it requires a substrate that can be radiolabelled with sufficient yield and specific activity that also has the right attributes for hyperpolarization. Dual PET/MRI can provide complementary information, enhancing the information content of both imaging modalities. For example arterial input functions can be derived from dynamic contrast enhanced MRI, which may be extrapolated to dynamic PET data providing an alternative to arterial sampling [109]. In an implanted colon tumor model, increased cell proliferation, determined using PET measurements of [^{18}F]FLT uptake, were correlated with regions of increased perfusion, detected using dynamic contrast agent enhanced MRI [108].

Preclinical imaging studies have been conducted largely in subcutaneous or orthotopic cancer cell line models, usually because of convenience and cost. However, these models only recapitulate certain aspects of tumor development and may not always be relevant to the clinic. The capability of pre-clinical imaging to answer questions about tumor biology would be much improved by the use of more advanced animal models [110]. These include spontaneous and conditional genetically engineered mouse models, tumors generated by somatic cell transduction [111, 112], patient-derived xenografts [113], embryonic stem cell chimeras [114] and orthotopically implanted organoids [115], which can capture the heterogeneity and diversity of human cancers [116].

Recent years have seen the development of several novel substrates for PET that has added substantially to the arsenal of more established radiotracers for imaging tumor metabolism. While many of these may not translate into routine clinical use they will undoubtedly have a role to play in experimental investigations of tumor cell metabolism and also in the drug development process, where they may be useful in making go/no go decisions in early stage clinical trials. For the more established radiotracers that are already in use, particularly FDG, there may be significant benefit in combining PET with other imaging modalities. PET/CT is already widely used and the use of PET/MRI is increasing, where metabolic imaging with PET can be combined with the numerous contrast mechanisms available in MRI to ask more specific questions about the regional metabolism of tumors. For example, low FDG uptake in a part of a tumor may indicate a low viable cell density or low FDG uptake by tumor cells in that region. Diffusion-weighted MRI, which can be used to estimate cell density, could potentially answer this question [2].

References

1. Gambhir SS. Molecular imaging of cancer with positron emission tomography. Nat Rev Cancer. 2002; 2(9):683–93. [PubMed: 12209157]
2. Brindle K. New approaches for imaging tumour responses to treatment. Nat Rev Cancer. 2008; 8(2): 94–107. [PubMed: 18202697]
3. Huang C, McConathy J. Radiolabeled amino acids for oncologic imaging. J Nucl Med. 2013; 54(7): 1007–10. [PubMed: 23708197]
4. Pruim J, et al. Brain tumors: L-[1-C-11]tyrosine PET for visualization and quantification of protein synthesis rate. Radiology. 1995; 197(1):221–6. [PubMed: 7568827]
5. Lewis DY, et al. Late Imaging with [1-^{11}C]Acetate Improves Detection of Tumor Fatty Acid Synthesis with PET. J Nucl Med. 2014; 55(7):1144–1149. [PubMed: 24777291]
6. Vavere AL, et al. 1-^{11}C-acetate as a PET radiopharmaceutical for imaging fatty acid synthase expression in prostate cancer. J Nucl Med. 2008; 49(2):327–34. [PubMed: 18199615]
7. Soloviev D, et al. [^{18}F]FLT: an imaging biomarker of tumour proliferation for assessment of tumour response to treatment. Eur J Cancer. 2012; 48(4):416–24. [PubMed: 22209266]
8. Tomasi G, Aboagye EO. Introduction to the analysis of PET data in oncology. J Pharmacokinet Pharmacodyn. 2013; 40(4):419–36. [PubMed: 23443280]
9. Tomasi G, Turkheimer F, Aboagye E. Importance of quantification for the analysis of PET data in oncology: review of current methods and trends for the future. Mol Imaging Biol. 2012; 14(2):131–46. [PubMed: 21842339]
10. Schwaiger M, Wester HJ. How many PET tracers do we need? J Nucl Med. 2011; 52:36S–41S. [PubMed: 22144553]
11. Gallagher FA, et al. Hyperpolarized ^{13}C MRI and PET: In Vivo Tumor Biochemistry. J Nucl Med. 2011; 52(9):1333–6. [PubMed: 21849405]

12. Waterton JC, Pylkkanen L. Qualification of imaging biomarkers for oncology drug development. Eur J Cancer. 2012; 48(4):409–15. [PubMed: 22226478]
13. Molecular Imaging and Contrast Agent Database (MICAD) [Internet]. National Center for Biotechnology Information (US); Bethesda (MD): 2004-2013. Available from: http://www.ncbi.nlm.nih.gov/books/NBK5330/
14. Di Chiro G, et al. Glucose utilization of cerebral gliomas measured by [^{18}F] fluorodeoxyglucose and positron emission tomography. Neurology. 1982; 32(12):1323–9. [PubMed: 6983044]
15. Lunt SY, Vander Heiden MG. Aerobic glycolysis: meeting the metabolic requirements of cell proliferation. Annu Rev Cell Dev Biol. 2011; 27:441–64. [PubMed: 21985671]
16. Pedersen P. Warburg, me and Hexokinase 2: Multiple discoveries of key molecular events underlying one of cancers' most common phenotypes, the "Warburg Effect", i.e., elevated glycolysis in the presence of oxygen. J Bioenerg Biomembr. 2007; 39(3):211–222. [PubMed: 17879147]
17. DeBerardinis RJ, et al. Beyond aerobic glycolysis: transformed cells can engage in glutamine metabolism that exceeds the requirement for protein and nucleotide synthesis. Proc Natl Acad Sci U S A. 2007; 104(49):19345–50. [PubMed: 18032601]
18. Rodrigues TB, et al. Magnetic resonance imaging of tumor glycolysis using hyperpolarized ^{13}C-labeled glucose. Nature Medicine. 2014; 20(1):93–7.
19. Fletcher JW, et al. Recommendations on the use of ^{18}F-FDG PET in oncology. J Nucl Med. 2008; 49(3):480–508. [PubMed: 18287273]
20. Furumoto S, et al. In vitro and in vivo characterization of 2-deoxy-2-^{18}F-fluoro-$_{D}$-mannose as a tumor-imaging agent for PET. J Nucl Med. 2013; 54(8):1354–1361. [PubMed: 23843565]
21. Arumugam T, et al. Preliminary evaluation of 1′-[^{18}F]fluoroethyl-b-D-lactose ([^{18}F]FEL) for detection of pancreatic cancer in nude mouse orthotopic xenografts. Nucl Med Biol. 2014; 41(10): 833–840. [PubMed: 25189831]
22. Wuest M, et al. Radiopharmacological evaluation of 6-deoxy-6-[^{18}F]fluoro-D-fructose as a radiotracer for PET imaging of GLUT5 in breast cancer. Nucl Med Biol. 2011; 38(4):461–75. [PubMed: 21531283]
23. Sorensen M, et al. The potential use of 2-[^{18}F]fluoro-2-deoxy-D-galactose as a PET/CT tracer for detection of hepatocellular carcinoma. Eur J Nucl Med Mol Imaging. 2011; 38(9):1723–31. [PubMed: 21553087]
24. Fukushima N, et al. Gene expression alterations in the non-neoplastic parenchyma adjacent to infiltrating pancreatic ductal adenocarcinoma. Mod Pathol. 2005; 18(6):779–87. [PubMed: 15791284]
25. Demaugre F, et al. HIP/PAP, a C-type lectin overexpressed in hepatocellular carcinoma, binds the RII alpha regulatory subunit of cAMP-dependent protein kinase and alters the cAMP-dependent protein kinase signalling. Eur J Biochem. 2004; 271(19):3812–20. [PubMed: 15373827]
26. Witney TH, et al. A comparison between radiolabeled fluorodeoxyglucose uptake and hyperpolarized ^{13}C-labeled pyruvate utilization as methods for detecting tumor response to treatment. Neoplasia. 2009; 11(6):574–82. [PubMed: 19484146]
27. Gowrishankar G, et al. GLUT 5 is not over-expressed in breast cancer cells and patient breast cancer tissues. PLoS One. 2011; 6(11):e26902. [PubMed: 22073218]
28. Smith TA. The rate-limiting step for tumor [^{18}F]fluoro-2-deoxy-D-glucose (FDG) incorporation. Nucl Med Biol. 2001; 28(1):1–4. [PubMed: 11182558]
29. Carroll L, Witney TH, Aboagye EO. Design and synthesis of novel ^{18}F-radiolabelled glucosamine derivatives for cancer imaging. MedChemComm. 2013; 4(4):653–656.
30. Witney TH, et al. A novel radiotracer to image glycogen metabolism in tumors by positron emission tomography. Cancer Res. 2014; 74(5):1319–28. [PubMed: 24590807]
31. Lai K, Klapa MI. Alternative pathways of galactose assimilation: could inverse metabolic engineering provide an alternative to galactosemic patients? Metab Eng. 2004; 6(3):239–244. [PubMed: 15256214]
32. Stincone A, et al. The return of metabolism: biochemistry and physiology of the pentose phosphate pathway. Biol Rev. 2014 doi:10.1111/brv.12140.

33. Clark PM, et al. Positron emission tomography probe demonstrates a striking concentration of ribose salvage in the liver. Proc Natl Acad Sci U S A. 2014; 111(28):E2866–74. [PubMed: 24982199]
34. Fischman AJ, et al. Muscle protein synthesis by positron-emission tomography with l-[methyl-^{11}C]methionine in adult humans. Proc Natl Acad Sci U S A. 1998; 95(22):12793–12798. [PubMed: 9788993]
35. Hawkins RA, et al. Estimation of Local Cerebral Protein Synthesis Rates with L-[l-^{11}C]Leucine and PET: Methods, Model, and Resultsin Animals and Humans. J Cereb Blood Flow Metab. 1989; 9(4):446–460. [PubMed: 2786885]
36. Plaat B, et al. Protein synthesis rate measured with l-[1-^{11}C]tyrosine positron emission tomography correlates with mitotic activity and MIB-1 antibody-detected proliferation in human soft tissue sarcomas. Eur J Nucl Med Mol Imaging. 1999; 26(4):328–332.
37. van den Bergh AC, et al. Tyrosine positron emission tomography and protein synthesis rate in pituitary adenoma: different effects of surgery and radiation therapy. Radiother Oncol. 2011; 98(2):213–6. [PubMed: 21296442]
38. Bustany P, et al. Brain tumor protein synthesis and histological grades: A study by positron emission tomography (PET) with C11-L-Methionine. Journal of Neuro-Oncology. 1986; 3(4): 397–404. [PubMed: 3485705]
39. Weber WA, et al. O-(2-[^{18}F]fluoroethyl)-L-tyrosine and L-[methyl-^{11}C]methionine uptake in brain tumours: initial results of a comparative study. Eur J Nucl Med Mol Imaging. 2000; 27(5): 542–9.
40. Becherer A, et al. Brain tumour imaging with PET: a comparison between [^{18}F]fluorodopa and [^{11}C]methionine. Eur J Nucl Med Mol Imaging. 2003; 30(11):1561–7. [PubMed: 14579097]
41. Nawashiro H, et al. L-type amino acid transporter 1 as a potential molecular target in human astrocytic tumors. Int J Cancer. 2006; 119(3):484–92. [PubMed: 16496379]
42. Betsunoh H, et al. Increased expression of system large amino acid transporter (LAT)-1 mRNA is associated with invasive potential and unfavorable prognosis of human clear cell renal cell carcinoma. BMC Cancer. 2013; 13:509. [PubMed: 24168110]
43. Kaira K, et al. Prognostic significance of L-type amino-acid transporter 1 expression in surgically resected pancreatic cancer. Br J Cancer. 2012; 107(4):632–8. [PubMed: 22805328]
44. Takeuchi K, et al. LAT1 expression in non-small-cell lung carcinomas: analyses by semiquantitative reverse transcription-PCR (237 cases) and immunohistochemistry (295 cases). Lung Cancer. 2010; 68(1):58–65. [PubMed: 19559497]
45. Floeth FW, et al. Prognostic Value of ^{18}F-Fluoroethyl-L-Tyrosine PET and MRI in Small Nonspecific Incidental Brain Lesions. J Nucl Med. 2008; 49(5):730–737. [PubMed: 18413396]
46. Piroth MD, et al. Prognostic value of early [^{18}F]fluoroethyltyrosine positron emission tomography after radiochemotherapy in glioblastoma multiforme. Int J Radiat Oncol Biol Phys. 2011; 80(1): 176–84. [PubMed: 20646863]
47. Weckesser M, et al. O-(2-[^{18}F]fluorethyl)-L -tyrosine PET in the clinical evaluation of primary brain tumours. Eur J Nucl Med Mol Imaging. 2005; 32(4):422–429. [PubMed: 15650870]
48. Kaira K, et al. Clinicopathological significance of ASC amino acid transporter-2 expression in pancreatic ductal carcinoma. Histopathology. 2015; 66(2):234–43. [PubMed: 24845232]
49. Shimizu K, et al. ASC amino-acid transporter 2 (ASCT2) as a novel prognostic marker in non-small cell lung cancer. Br J Cancer. 2014; 110(8):2030–9. [PubMed: 24603303]
50. Fuchs BC, Bode BP. Amino acid transporters ASCT2 and LAT1 in cancer: partners in crime? Semin Cancer Biol. 2005; 15(4):254–66. [PubMed: 15916903]
51. Nanni C, et al. ^{18}F-FACBC compared with ^{11}C-choline PET/CT in patients with biochemical relapse after radical prostatectomy: a prospective study in 28 patients. Clin Genitourin Cancer. 2014; 12(2):106–10. [PubMed: 24135632]
52. Turkbey B, et al. Localized prostate cancer detection with ^{18}F-FACBC PET/CT: comparison with MR imaging and histopathologic analysis. Radiology. 2014; 270(3):849–56. [PubMed: 24475804]
53. Yu W, et al. Synthesis, radiolabeling, and biological evaluation of (R)- and (S)-2-amino-3-[^{18}F]fluoro-2-methylpropanoic acid (FAMP) and (R)- and (S)-3-[^{18}F]fluoro-2-methyl-2-N-

(methylamino)propanoic acid (NMeFAMP) as potential PET radioligands for imaging brain tumors. J Med Chem. 2010; 53(2):876–86. [PubMed: 20028004]

54. Yu W, et al. System a amino acid transport-targeted brain and systemic tumor PET imaging agents 2-amino-3-[(18)F]fluoro-2-methylpropanoic acid and 3-[(18)F]fluoro-2-methyl-2-(methylamino)propanoic acid. Nucl Med Biol. 2015; 42(1):8–18. [PubMed: 25263130]
55. Webster JM, et al. Functional imaging of oxidative stress with a novel PET imaging agent, ^{18}F-5-fluoro-L-aminosuberic acid. J Nucl Med. 2014; 55(4):657–64. [PubMed: 24578242]
56. Krasikova RN, et al. 4-[^{18}F]Fluoroglutamic Acid (BAY 85-8050), a New Amino Acid Radiotracer for PET Imaging of Tumors: Synthesis and in Vitro Characterization. J Med Chem. 2011; 54(1): 406–410. [PubMed: 21128591]
57. Ploessl K, et al. Comparative Evaluation of ^{18}F-Labeled Glutamic Acid and Glutamine as Tumor Metabolic Imaging Agents. Journal of Nuclear Medicine. 2012; 53(10):1616–1624. [PubMed: 22935578]
58. Koglin N, et al. Specific PET Imaging of x_C^- Transporter Activity Using a ^{18}F-Labeled Glutamate Derivative Reveals a Dominant Pathway in Tumor Metabolism. Clin Cancer Res. 2011; 17(18): 6000–6011. [PubMed: 21750203]
59. Baek S, et al. (4S)-4-(3-^{18}F-fluoropropyl)-L-glutamate for imaging of x_C transporter activity in hepatocellular carcinoma using PET: preclinical and exploratory clinical studies. J Nucl Med. 2013; 54(1):117–23. [PubMed: 23232273]
60. Baek S, et al. Exploratory clinical trial of (4S)-4-(3-[^{18}F]fluoropropyl)-L-glutamate for imaging x_C^- transporter using positron emission tomography in patients with non-small cell lung or breast cancer. Clin Cancer Res. 2012; 18(19):5427–37. [PubMed: 22893629]
61. Lu SC. Regulation of hepatic glutathione synthesis: current concepts and controversies. FASEB J. 1999; 13(10):1169–83. [PubMed: 10385608]
62. Lewerenz J, et al. The cystine/glutamate antiporter system x_c^- in health and disease: from molecular mechanisms to novel therapeutic opportunities. Antioxid Redox Signal. 2013; 18(5): 522–55. [PubMed: 22667998]
63. Ishimoto T, et al. CD44 variant regulates redox status in cancer cells by stabilizing the xCT subunit of system x_c^- and thereby promotes tumor growth. Cancer Cell. 2011; 19(3):387–400. [PubMed: 21397861]
64. Wise DR, et al. Myc regulates a transcriptional program that stimulates mitochondrial glutaminolysis and leads to glutamine addiction. Proc Natl Acad Sci U S A. 2008; 105(48):18782–7. [PubMed: 19033189]
65. Qu W, et al. Preparation and characterization of L-[5-^{11}C]-glutamine for metabolic imaging of tumors. J Nucl Med. 2012; 53(1):98–105. [PubMed: 22173839]
66. Wu F, et al. Uptake of ^{14}C- and ^{11}C-labeled glutamate, glutamine and aspartate in vitro and in vivo. Anticancer Res. 2000; 20(1A):251–6. [PubMed: 10769663]
67. Lieberman BP, et al. PET imaging of glutaminolysis in tumors by ^{18}F-(2S,4R)4-fluoroglutamine. J Nucl Med. 2011; 52(12):1947–55. [PubMed: 22095958]
68. Venneti S, et al. Glutamine-based PET imaging facilitates enhanced metabolic evaluation of gliomas in vivo. Sci Transl Med. 2015; 7(274):274ra17.
69. Wu Z, et al. [^{18}F](2S,4S)-4-(3-Fluoropropyl)glutamine as a tumor imaging agent. Mol Pharm. 2014; 11(11):3852–66. [PubMed: 25095908]
70. Bozza PT, Viola JPB. Lipid droplets in inflammation and cancer. Prostaglandins Leukot Essent Fatty Acids. 2010; 82(4-6):243–250. [PubMed: 20206487]
71. Carracedo A, Cantley LC, Pandolfi PP. Cancer metabolism: fatty acid oxidation in the limelight. Nat Rev Cancer. 2013; 13(4):227–232. [PubMed: 23446547]
72. DeBerardinis RJ, et al. Brick by brick: metabolism and tumor cell growth. Curr Opin Genet Dev. 2008; 18(1):54–61. [PubMed: 18387799]
73. Iozzo P, et al. Fatty Acid Metabolism in the Liver, Measured by Positron Emission Tomography, Is Increased in Obese Individuals. Gastroenterology. 2010; 139(3):846–856. [PubMed: 20685204]
74. Pandey MK, Bansal A, DeGrado TR. Fluorine-18 labeled thia fatty acids for PET imaging of fatty acid oxidation in heart and cancer. Heart Metab. 2011; 51:15–19.

75. DeGrado TR, et al. Synthesis and preliminary evaluation of 18-^{18}F-fluoro-4-thia-oleate as a PET probe of fatty acid oxidation. J Nucl Med. 2010; 51(8):1310–7. [PubMed: 20660391]
76. Daniëls VW, et al. Cancer Cells Differentially Activate and Thrive on De Novo Lipid Synthesis Pathways in a Low-Lipid Environment. PLoS One. 2014; 9(9):e106913. [PubMed: 25215509]
77. Mashimo T, et al. Acetate Is a Bioenergetic Substrate for Human Glioblastoma and Brain Metastases. Cell. 2014; 159(7):1603–1614. [PubMed: 25525878]
78. Lyssiotis, Costas A.; Cantley, Lewis C. Acetate Fuels the Cancer Engine. Cell. 2014; 159(7):1492–1494. [PubMed: 25525870]
79. Yoshii Y, et al. Tumor uptake of radiolabeled acetate reflects the expression of cytosolic acetyl-CoA synthetase: implications for the mechanism of acetate PET. Nucl Med Biol. 2009; 36(7):771–7. [PubMed: 19720289]
80. Nishii R, et al. Pharmacokinetics, Metabolism, Biodistribution, Radiation Dosimetry, and Toxicology of ^{18}F-Fluoroacetate (^{18}F-FACE) in Non-human Primates. Mol Imaging Biol. 2012; 14(2):213–224. [PubMed: 21437735]
81. Lindhe O, et al. [^{18}F]Fluoroacetate is not a functional analogue of [^{11}C]acetate in normal physiology. Eur J Nucl Med Mol Imaging. 2009; 36(9):1453–9. [PubMed: 19387639]
82. Pillarsetty N, Punzalan B, Larson SM. 2-^{18}F-Fluoropropionic Acid as a PET Imaging Agent for Prostate Cancer. J Nucl Med. 2009; 50(10):1709–1714. [PubMed: 19759108]
83. Pisaneschi F, et al. Synthesis of [^{18}F]fluoro-pivalic acid: an improved PET imaging probe for the fatty acid synthesis pathway in tumours. MedChemComm. 2013; 4(10):1350–1353.
84. Witney TH, et al. Preclinical Evaluation of 3-^{18}F-Fluoro-2,2-Dimethylpropionic Acid as an Imaging Agent for Tumor Detection. J Nucl Med. 2014; 55(9):1506–1512. [PubMed: 25012458]
85. DeGrado TR, et al. Synthesis and evaluation of ^{18}F-labeled choline as an oncologic tracer for positron emission tomography: initial findings in prostate cancer. Cancer Res. 2001; 61(1):110–7. [PubMed: 11196147]
86. Umbehr MH, et al. The role of ^{11}C-choline and ^{18}F-fluorocholine positron emission tomography (PET) and PET/CT in prostate cancer: a systematic review and meta-analysis. Eur Urol. 2013; 64(1):106–17. [PubMed: 23628493]
87. de Vogel S, et al. Sarcosine and other metabolites along the choline oxidation pathway in relation to prostate cancer—A large nested case-control study within the JANUS cohort in Norway. Int J Cancer. 2014; 134(1):197–206. [PubMed: 23797698]
88. Gibellini F, Smith TK. The Kennedy pathway—De novo synthesis of phosphatidylethanolamine and phosphatidylcholine. IUBMB Life. 2010; 62(6):414–428. [PubMed: 20503434]
89. Witney TH, et al. Evaluation of deuterated ^{18}F- and ^{11}C-labeled choline analogs for cancer detection by positron emission tomography. Clin Cancer Res. 2012; 18(4):1063–72. [PubMed: 22235095]
90. Smith G, et al. Radiosynthesis and pre-clinical evaluation of [^{18}F]fluoro-[1,2-^{2}H$_4$]choline. Nucl Med Biol. 2011; 38(1):39–51. [PubMed: 21220128]
91. Challapalli A, et al. Biodistribution and radiation dosimetry of deuterium-substituted ^{18}F-fluoromethyl-[1, 2-^{2}H$_4$]choline in healthy volunteers. J Nucl Med. 2014; 55(2):256–63. [PubMed: 24492392]
92. Locasale JW. Serine, glycine and one-carbon units: cancer metabolism in full circle. Nat Rev Cancer. 2013; 13(8):572–583. [PubMed: 23822983]
93. Jain M, et al. Metabolite Profiling Identifies a Key Role for Glycine in Rapid Cancer Cell Proliferation. Science. 2012; 336(6084):1040–1044. [PubMed: 22628656]
94. Nakajima EC, Van Houten B. Metabolic symbiosis in cancer: refocusing the Warburg lens. Mol Carcinog. 2013; 52(5):329–37. [PubMed: 22228080]
95. Tedeschi PM, et al. Contribution of serine, folate and glycine metabolism to the ATP, NADPH and purine requirements of cancer cells. Cell Death Dis. 2013; 4:e877. [PubMed: 24157871]
96. Cantor JR, Sabatini DM. Cancer cell metabolism: one hallmark, many faces. Cancer Discov. 2012; 2(10):881–98. [PubMed: 23009760]
97. Brooks GA. Cell-cell and intracellular lactate shuttles. J Physiol. 2009; 587(23):5591–5600. [PubMed: 19805739]

98. Rajagopalan KN, DeBerardinis RJ. Role of glutamine in cancer: therapeutic and imaging implications. J Nucl Med. 2011; 52(7):1005–8. [PubMed: 21680688]
99. Phang JM. The proline regulatory axis and cancer. Front Oncol. 2012; 2
100. Gunn RN, Gunn SR, Cunningham VJ. Positron emission tomography compartmental models. J Cereb Blood Flow Metab. 2001; 21(6):635–52. [PubMed: 11488533]
101. Tomasi G, et al. Double-input compartmental modeling and spectral analysis for the quantification of positron emission tomography data in oncology. Phys Med Biol. 2012; 57(7): 1889–906. [PubMed: 22421332]
102. Mori Y, et al. Improved spillover correction model to quantify myocardial blood flow by ^{11}C-acetate PET: comparison with ^{15}O-H_2O PET. Ann Nucl Med. 2015; 29(1):15–20. [PubMed: 25209232]
103. van den Hoff J, et al. A kinetic model for cardiac PET with [1-carbon-11]-acetate. J Nucl Med. 1996; 37(3):521–9. [PubMed: 8772659]
104. Schiepers C, et al. 1-^{11}C-acetate kinetics of prostate cancer. J Nucl Med. 2008; 49(2):206–15. [PubMed: 18199613]
105. Brindle KM, et al. Tumor imaging using hyperpolarized ^{13}C magnetic resonance spectroscopy. Magn Reson Med. 2011; 66(2):505–19. [PubMed: 21661043]
106. Comment A, Merritt ME. Hyperpolarized magnetic resonance as a sensitive detector of metabolic function. Biochemistry. 2014; 53(47):7333–57. [PubMed: 25369537]
107. Nelson SJ, et al. Metabolic Imaging of Patients with Prostate Cancer Using Hyperpolarized 1-C-13 Pyruvate. Sci Transl Med. 2013; 5(198):10.
108. Judenhofer MS, et al. Simultaneous PET-MRI: a new approach for functional and morphological imaging. Nat Med. 2008; 14(4):459–65. [PubMed: 18376410]
109. Poulin E, et al. Conversion of arterial input functions for dual pharmacokinetic modeling using Gd-DTPA/MRI and ^{18}F-FDG/PET. Magn Reson Med. 2013; 69(3):781–92. [PubMed: 22570280]
110. Frese KK, Tuveson DA. Maximizing mouse cancer models. Nat Rev Cancer. 2007; 7(9):645–58. [PubMed: 17687385]
111. Cho H, et al. RapidCaP, a novel GEM model for metastatic prostate cancer analysis and therapy, reveals myc as a driver of Pten-mutant metastasis. Cancer Discov. 2014; 4(3):318–33. [PubMed: 24444712]
112. Rodriguez E, et al. Versatile and enhanced tumour modelling in mice via somatic cell transduction. J Pathol. 2014; 232(4):449–57. [PubMed: 24307564]
113. Tentler JJ, et al. Patient-derived tumour xenografts as models for oncology drug development. Nat Rev Clin Oncol. 2012; 9(6):338–50. [PubMed: 22508028]
114. Huijbers IJ, et al. Rapid target gene validation in complex cancer mouse models using re-derived embryonic stem cells. EMBO Mol Med. 2014; 6(2):212–25. [PubMed: 24401838]
115. Boj SF, et al. Organoid models of human and mouse ductal pancreatic cancer. Cell. 2015; 160(1-2):324–38. [PubMed: 25557080]
116. Politi K, Pao W. How genetically engineered mouse tumor models provide insights into human cancers. J Clin Oncol. 2011; 29(16):2273–81. [PubMed: 21263096]
117. Passarella S, et al. Mitochondria and l-lactate metabolism. FEBS Letters. 2008; 582(25-26):3569–3576. [PubMed: 18831974]
118. Carroll L, et al. Radiosynthesis and in vivo tumor uptake of 2-deoxy-2-[^{18}F] fluoro-myo-inositol. Bioorg Med Chem Lett. 2012; 22(19):6148–6150. [PubMed: 22944120]
119. Dunet V, et al. Performance of ^{18}F-fluoro-ethyl-tyrosine (^{18}F-FET) PET for the differential diagnosis of primary brain tumor: a systematic review and Metaanalysis. J Nucl Med. 2012; 53(2):207–14. [PubMed: 22302961]
120. Lapa C, et al. Comparison of the amino acid tracers ^{18}F-FET and ^{18}F-DOPA in high-grade glioma patients. J Nucl Med. 2014; 55(10):1611–6. [PubMed: 25125481]
121. Wiriyasermkul P, et al. Transport of 3-fluoro-L-alpha-methyl-tyrosine by tumor-upregulated L-type amino acid transporter 1: a cause of the tumor uptake in PET. J Nucl Med. 2012; 53(8): 1253–61. [PubMed: 22743251]

122. Prenant C, et al. Carbon-11 labelled analogs of alanine by the strecker synthesis. J Labelled Comp Radiopharm. 1995; 36(6):579–586.

123. Kit S, Greenberg DM. Tracer studies on the metabolism of the Gardner lymphosarcoma. III. The rate of radioactive alanine and glycine uptake into the protein of lymphosarcoma cells and normal spleen cells. Cancer Res. 1951; 11(7):500–4. [PubMed: 14848818]

124. Wang L, et al. Synthesis and evaluation of ^{18}F labeled alanine derivatives as potential tumor imaging agents. Nucl Med Biol. 2012; 39(7):933–943. [PubMed: 22542392]

125. Muller A, et al. Imaging tumour $ATB^{0,+}$ transport activity by PET with the cationic amino acid O-2((2-[^{18}F]fluoroethyl)methyl-amino)ethyltyrosine. Mol Imaging Biol. 2014; 16(3):412–20. [PubMed: 24307544]

126. Mitsuoka K, et al. Cancer detection using a PET tracer, ^{11}C-glycylsarcosine, targeted to H^+/peptide transporter. J Nucl Med. 2008; 49(4):615–22. [PubMed: 18344442]

127. Turkman N, Gelovani JG, Alauddin MM. Radiosynthesis of N5-[^{18}F]fluoroacetylornithine (N5-[^{18}F]FAO) for PET imaging of ornithine decarboxylase (ODC) in malignant tumors. J Labelled Comp Radiopharm. 2011; 54(1):33–37.

128. Angsten G, et al. Inhibition of carnitine-acyl transferase I by oxfenicine studied in vivo with [^{11}C]-labeled fatty acids. Nucl Med Biol. 2005; 32(5):495–503. [PubMed: 15982580]

Europe PMC Funders Author Manuscripts

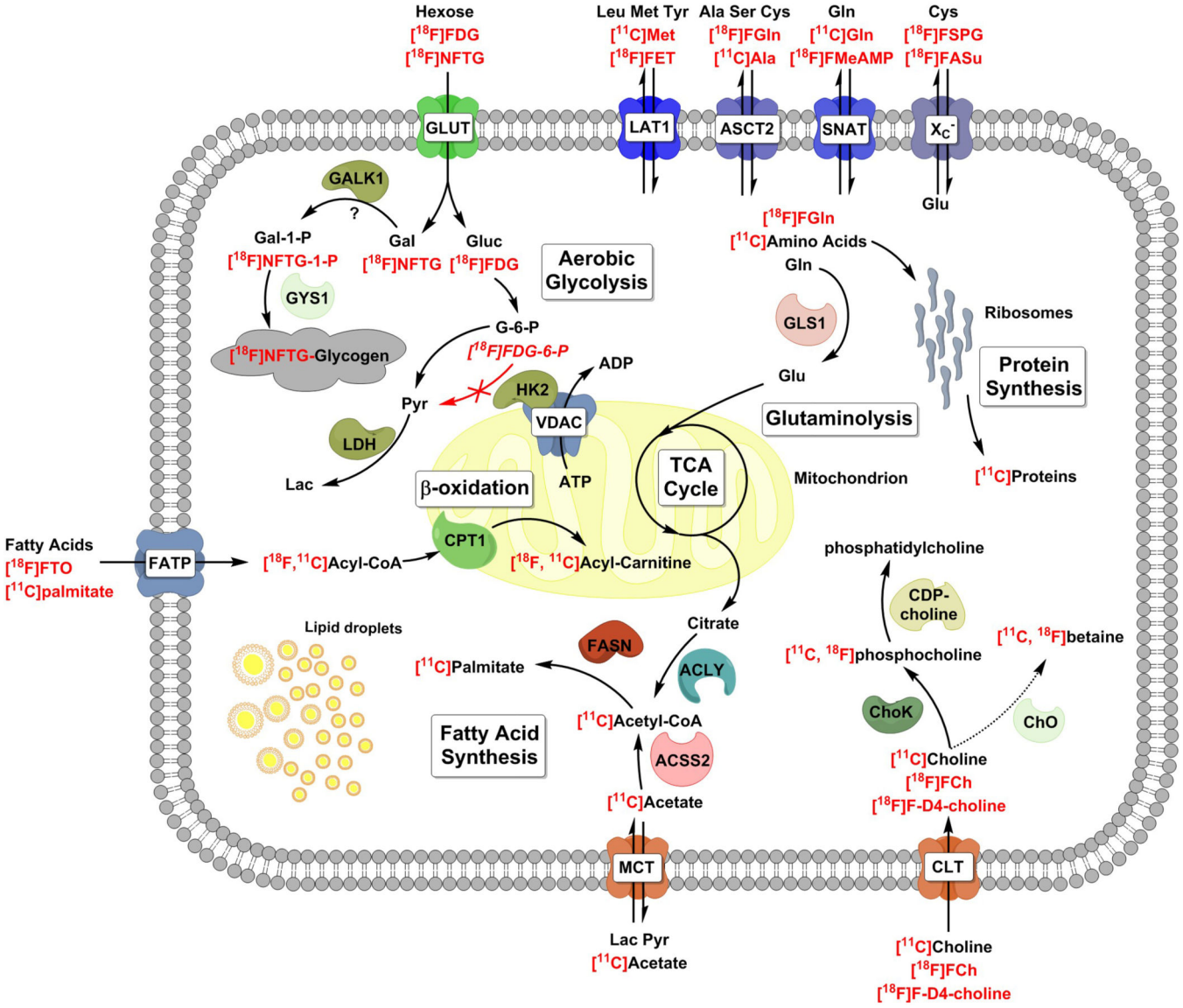

Figure 1.

A schematic of the metabolic pathways and enzymes responsible for the intracellular trapping of key PET substrates for imaging cancer metabolism. Radionuclides and PET substrates are shown in red. Note the localization of hexokinase 2 (HK2) to the mitochondria [16]. When the tumor cell activates aerobic glycolysis, HK2 can bind to the anion transporter channel on the outer mitochondrial membrane (VDAC), preferentially gaining access to mitochondrially generated ATP [117]. ACLY – ATP citrate lyase; ACSS2 – acetyl coA synthetase short-chain family member 2, cytosolic; ASCT2 - neutral amino acid transporter (SLC1A5); Ala – alanine; CPT1 – carnitine palmitoyl transferase I; CTL – choline transporter–like proteins (SLC44A); Cys – cysteine; FASN – fatty acid synthase; FATP – fatty acid transport protein; Gal – galactose; GALK1 – galactokinase 1; GLS1 – glutaminase 1; Gluc – glucose; Gln – glutamine; Glu – glutamate; GLUT – glucose transporter; GYS1 – UDP-glucose-glycogen glucosyltransferase; HK2 – hexokinase 2;

LAT1 - L-type amino acid transporter 1 (SLC7A5); LDH – lactate dehydrogenase; MCT monocarboxylate transporter; SNAT – system A amino acid transporter; X_C^- – anionic amino acid transporter light chain, system x_c^- (SLC7A11); TCA – tricarboxylic acid cycle; VDAC – voltage-dependent anion channel

Europe PMC Funders Author Manuscripts

Table1

PET tracers used for imaging cancer metabolism and their purported target transporters and enzymes. ACSS2 – acetyl coAsynthetase short-chain family member 2, cytosolic; ASCT2 – neutral amino acid transporter (SLC1A5); $ATB^{0,+}$ – amino acid transporter ATBO (SLC6A14); ChoK – choline kinase; ChO – choline oxidase; EAAT – excitatory amino-acid transporter; FA – fatty acid; FASN – fatty acid synthase; GLUT – glucose transporter; GYS1 – UDP-glucose-glycogen glucosyltransferase; HIP/PAP – hepatocarcinoma-intestine-pancreas/pancreatitis-associated protein; HK – hexokinase; KHK – ketohexokinase; LAT1 - L-type amino acid transporter 1 (SLC7A5); ODC – ornithine decarboxylase; PEPT1 – Peptide transporter 1 (SLC15A1); SMIT – sodium/myo-Inositol transporter; SNAT – system A amino acid transporter; X_C^- – anionic amino acid transporter light chain, system X_c^- (SLC7A11)

Carbohydrates	***Target***	***Ref***
2-[^{18}F]-Fluoro-2-deoxy- D –glucose (FDG)	GLUT-1,3, HK	[19]
2-deoxy-2-[^{18}F]fluoro-D-mannose lactose ([^{18}F]FDM)	GLUT-1,3, HK	[20]
2-[^{18}F]fluoro-2-deoxy-D-galactose ([^{18}F]FDGal)	GLUT-1,3, HK	[23]
6-deoxy-6-[^{18}F]fluoro-D-fructose ([^{18}F]FDF)	GLUT-5, KHK	[22]
1-[^{18}F]fluoroethyl-beta-D-lactose ([^{18}F]FEL)	HIP/PAP	[21]
2-deoxy-2-[^{18}F]fluoro-myo-inositol	SMIT	[118]
^{18}F-N-(methyl-(2-fluoroethyl)-1H-[1,2,3]triazole-4-yl)glucosamine ([^{18}F]NFTG)	GYS1	[29, 30]
Amino Acids		
[^{11}C]methionine	LAT1, protein synthesis	[34, 38]
[^{11}C]tyrosine	LAT1, protein synthesis	[37]
[^{11}C]leucine	LAT1, protein synthesis	[35]
[^{18}F] Fluoroethyltyrosine ([^{18}F]FET)	LAT1	[119]
[^{18}F]-Dihydroxy-phenyl-alanine ([^{18}F]FDOPA)	LAT1	[120]
L-3-^{18}F-α-methyl tyrosine ([^{18}F]FAMT)	LAT1	[121]
trans-1-amino-3-[18F]fluorocyclobutanecarboxylic acid (FACBC)	LAT1, ASCT2	[16]
^{18}F-4-fluoroglutamine	ASCT2	[57, 67]
[^{11}C]alanine	ASCT2	[122, 123]
[^{18}F]alanine	ASCT2	[124]
^{11}C-glutamine	SNAT, ASCT2	[62, 66]
(4S)-4-(3-^{18}F-fluoropropyl)-L-glutamate ([^{18}F]FSPG)	X_c^-	[58, 59]
^{18}F-5-Fluoro-L-Aminosuberic Acid ([^{18}F]FASu)	X_c^-	[55]
[18F](2S,4S)-4-(3-Fluoropropyl)glutamine	X_c^-	[58, 69]
^{18}F-4-fluoroglutamate (BAY 85-8050)	X_c^-, EAAT	[56, 57]
O-2((2-[18F]fluoroethyl)methyl-amino)ethyltyrosine	$ATB^{0,+}$	[125]
[^{11}Cglycylsarcosine (^{11}C-Gly-Sar)	PEPT1	[126]
N5-[^{18}F]fluoroacetylornithine (N5-[^{18}F]FAO)	ODC	[127]

Europe PMC Funders Author Manuscripts

Carbohydrates	***Target***	***Ref***
Fatty acids		
[^{11}C]acetate	FASN, ACSS2, FA synthesis	[5, 6, 79]
[^{11}C]choline	ChoK, ChO	[85]
[^{18}F]Fluorocholine ([^{18}F]FCh)	ChoK, ChO	[86]
[^{18}F]F-D4-choline	ChoK	[89, 90]
[^{18}F]fluoro-pivalic acid (FPIA)	β-oxidation	[84]
[^{11}C]palmitate	β-oxidation	[73, 128]
18-[^{18}F] fluoro-4-thia-oleate (FTO)	β-oxidation	[75]